JCTC Journal of Chemical Theory and Computation

Water's Contribution to the Energetic Roughness from Peptide Dynamics

Quentin Johnson,[†] Urmi Doshi,[†] Tongye Shen,[‡,§] and Donald Hamelberg*[,†]

Department of Chemistry and the Center for Biotechnology and Drug Design, Georgia State University, Atlanta, Georgia 30302-4098, Department of Biochemistry, Cellular & Molecular Biology, University of Tennessee, Knoxville, Tennessee 37996, and Center for Molecular Biophysics, Oak Ridge National Laboratory, Oak Ridge, Tennessee 37830

Received April 5, 2010

Abstract: Water plays a very important role in the dynamics and function of proteins. Apart from protein−protein and protein−water interactions, protein motions are accompanied by the formation and breakage of hydrogen-bonding network of the surrounding water molecules. This ordering and reordering of water also adds to the underlying roughness of the energy landscape of proteins and thereby alters their dynamics. Here, we extract the contribution of water to the ruggedness (in terms of an energy scale ε) of the energy landscape from molecular dynamics simulations of a peptide substrate analogue of prolyl *cis*−*trans* isomerases. In order to do so, we develop and implement a model based on the position space analog of the Ornstein−Uhlenbeck process and Zwanzig's theory of diffusion on a rough potential. This allows us to also probe an important property of the widely used atomistic simulation water models that directly affects the dynamics of biomolecular systems and highlights the importance of the choice of the water model in studying protein dynamics. We show that water contributes an additional roughness to the energy landscape. At lower temperatures this roughness, which becomes comparable to k_BT, can considerably slow down protein dynamics. These results also have much broader implications for the function of some classes of enzymes, since the landscape topology of their substrates may change upon moving from an aqueous environment into the binding site.

Introduction

The hyperdimensional energy landscape of biological macromolecules has a very complex topology representing self-assembly of their three-dimensional structures from unfolded states, their interactions with other partners, and conformational transitions for their function.[1,2] To add to the complexity, the surface of the landscape is not smooth but rather jagged with numerous local minima separated by energy barriers of different heights. These minima represent a vast number of conformational substates, each specified by the configuration of the biomolecule including its hydration shell (i.e., water molecules immediately surrounding the biomolecule) as well as the internal water molecules. Water thus constitutes an integral part of biomolecular structure.[1,3,4] As the biomolecule undergoes conformational switching between these substates, energy barriers arise due to the formation and breakage of unfavorable interactions within the biomolecule, between the biomolecule and water, and between water molecules. The unevenness of the energy landscape can lead to kinetic traps if it is comparable or much greater than k_BT, where k_B is the Boltzmann constant and T is the temperature. To highlight the nature of the inherent roughness of the energy landscape of biomolecules, theories have been developed[5−7] and for proteins, roughness has been estimated

* Corresponding author phone: (404)413-5564; fax: (404)413-5505; e-mail: dhamelberg@gsu.edu. Corresponding author address: Department of Chemistry, Georgia State University, Atlanta, GA 30302-4098.

[†] Georgia State University.

[‡] University of Tennessee.

[§] Oak Ridge National Laboratory.

10.1021/ct100183s
Published on Web 08/26/2010

experimentally.[6,8,9] From these studies the characteristic scale for roughness is estimated to fall in the range of few (i.e., ~2−5) k_BT at 25 °C.

The potential energy landscape of water is also rough with many minima, each typifying a different configuration of the hydrogen-bonding network. Therefore, water by itself has slow dynamics as the hydrogen-bonding network rearranges by breaking and forming hydrogen bonds.[10,11] The energetic component of hydrogen bond network rearrangements has been estimated to be between 0.8 and 1.5 kcal/mol using X-ray absorption spectroscopy.[12,13] This value represents the average thermal energy required to distort a hydrogen bond or to rearrange or change the fully coordinated configuration of water to a configuration with a broken hydrogen bond to the donor. However, the quality of the data and the interpretation of the results have been questioned.[14] The exact structure of liquid water and the average thermal energy associated with hydrogen bond rearrangements are still unresolved and involve areas of active research.[15−19] Nonetheless, reorientation of hydrogen bonds between water molecules around proteins will undoubtedly have an effect on the dynamics of proteins and will show up as an energetic component on the overall protein energy landscape.

Biomolecular motions, especially those that bring about conversions between different conformational substates and do not involve forming or breaking of any covalent bonds, are coupled to solvent fluctuations.[20,21] The role of water on protein dynamics has been studied extensively.[20−23] It has been suggested from spectroscopic studies that large-scale protein motions such as folding/unfolding or conformational changes associated with opening/closing of protein channels or accommodation of ligands are dampened by the fluctuations in the bulk solvent and therefore depend on solvent viscosity.[21] The water molecules in the hydration shell form a short-lived clathrate-like structure around the protein molecules. As proteins undergo constant thermal motions and conformational changes, the network of hydrogen bonds in the hydration shell rearranges. Breaking and reforming of these hydrogen bonds contribute to the overall roughness on the energy landscape of the protein and can restrict the motion of proteins, especially at lower temperatures. Besides, the effect of solvent viscosity, which is manifested as frictional drag and at the microscopic level as the dynamic network of hydrogen bonds in bulk water, also partly adds to the energetic roughness and impedes protein dynamics. In order to get a better insight into the function and dynamics of proteins, it is necessary to understand the nature of the roughness and calculate the magnitude of the different contributions to it. The magnitude of the roughness due to hydration on the energy landscape is not well characterized, and its effects on protein dynamics are less understood. A full understanding of this aspect of protein dynamics has broad implications, such as the dynamic effects of desolvated molecules relative to that of solvated molecules, the low-temperature behavior of solvated biomolecules, and the fundamental nature of water hydrogen bond network.

In the peptidyl prolyl *cis*−*trans* isomerases (PPIases) class of enzymes wherein the active site is very hydrophobic, the effect of moving the substrate from aqueous solvent to the active site of PPIases has been suggested to be a possible contributing factor to the catalytic activity.[23−25] PPIases catalyze the *cis*−*trans* isomerization of the peptide ω-bond preceding prolyl of protein backbone, and they function without any bond forming or breaking during the catalytic process.[23] *Cis*−*trans* isomerization of the prolyl ω-bond is the switching mechanism in several signaling pathways[26] and is important for protein folding.[27,28] The role of aqueous solvent, or the lack thereof, in PPIase catalytic activity is not well understood. Therefore, in the present work we investigate the effects of solvent on the dynamics of a peptide substrate analogue (Ace-Ala-Pro-Nme), focusing only on one torsional degree of freedom, i.e. the peptide bond dihedral (ω) preceding Pro. The ω-bond angle is a good reaction coordinate for describing the *cis*−*trans* isomerization.[29] We present here a novel approach to quantitatively capture the energetic effect of water on the roughness along the prolyl ω-bond angle. In the peptide substrate analogue, Ace-Ala-Pro-Nme, we observe the fluctuations of the ω dihedral preceding the Pro residue in the *trans* basin in all-atom molecular dynamics (MD) simulations with explicit water. We develop a model by describing the Brownian motion in a harmonic well as a position space analog of the Ornstein−Uhlenbeck process.[30] We then calculate the diffusion coefficients of the ω dihedral angle on an effective 1-D harmonic potential at different temperatures in the presence of each of the commonly used water models. Using the temperature dependence of these effective diffusion coefficients and the expression given by Zwanzig[5] that links the effective diffusion coefficient to roughness, we tease out the magnitude of the (energetic) roughness contributed by various water models. Additionally, we learn the extent to which the roughness provided by water influences the energy landscape and hence the peptide dynamics along the ω-bond angle degree of freedom. Since atomistic simulations are routinely used to extract dynamic information of biomolecules, knowing the effects of solvent on protein dynamics on a quantitative level will allow us to make a more informed choice of the water model to be used in MD studies, i.e. it will help in reproducing experimentally measured quantities of biomolecules better as well as in force field parametrization.

Results

Dynamics of the Protein Peptide ω-Bond Angle. During the course of the MD simulations of Ace-Ala-Pro-Nme (Figure 1, left panel) in explicit water using commonly used atomistic solvent models, we monitored the dynamics of the ω-bond angle (CA−C−N′−CA′). Shown in Figure 1 (right panel) are the fluctuations of the ω-dihedral in the *trans* basin, i.e. around 180°. For biomolecules, in general, the decay of the autocorrelation function of the velocity along a degree of freedom has a characteristic time scale that is much shorter than that of the displacement of that degree of freedom. Since this is also true for the ω-bond angle, we can describe the actual complicated motion of the peptide along the ω-bond angle as diffusive motion on an effective one-dimensional (1D) energy profile, $U(\omega)$. Such diffusive motion of the peptide on an

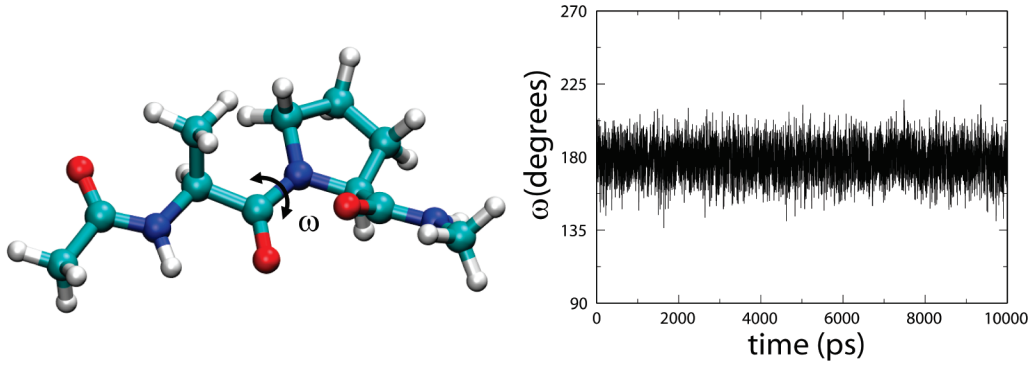

Figure 1. (left) Structure of Ace-Ala-Pro-Nme and (right) the fluctuations of the ω-bond angle between Ala and Pro during the simulation at 300 K in SPC/E water.

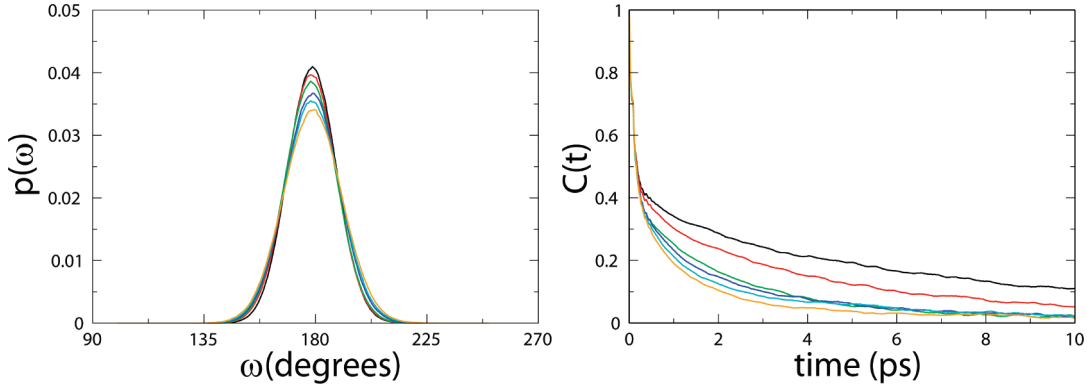

Figure 2. (left) The distribution of the peptide ω-bond angle between Ala and Pro in Ace-Ala-Pro-Nme at six different temperatures (275 K (black), 300 K (red), 325 K (green), 350 K (blue), 375 K (cyan), and 400 K (orange)) in SPC/E water. (right) Autocorrelation function of ω at the same six temperatures as in the left panel.

effective 1D energy profile is generally described by the Smoluchowski equation

$$\frac{\partial p(\omega,t)}{\partial t} = D\frac{\partial}{\partial \omega}\left[\frac{\partial p(\omega,t)}{\partial \omega} + \frac{p(\omega,t)}{k_B T}\frac{\partial U(\omega)}{\partial \omega}\right] \quad (1)$$

where $p(\omega,t)$ is the time-dependent probability distribution of the peptide ω-bond angle, and the diffusion coefficient D is assumed to be independent of ω.

As can be seen from Figure 2, the probability distribution of the ω-bond angle in the *trans* basin is approximately Gaussian. Therefore, the effective 1D potential landscape, $U(\omega)$, of the motion of the peptide along the ω-bond angle in the *trans* basin can be approximated as a harmonic potential $U(\omega) = (K)/(2)(\omega - \gamma)^2$, where K is the effective spring constant and $\gamma \approx 180°$. Furthermore, the Brownian motion in a harmonic potential described as a position space analog of the Ornstein−Uhlenbeck (OU) process[30] has been studied extensively, and the autocorrelation function of ω is given by

$$C(t) = \frac{<\omega(0)\omega(t)>}{<\omega^2>} = \exp(-tDK/k_B T) \quad (2)$$

where

$$<\omega^2> = k_B T/K \quad (3)$$

The autocorrelation functions of ω at six different temperatures (275, 300, 325, 350, 375, and 400 K) calculated from the simulation data in the SPC/E water model are also shown in Figure 2 (right panel). By fitting the tail of the autocorrelation functions in Figure 2 using eqs 2 and 3 to a single exponential, we obtained D, the diffusion coefficient, of the displacement of the ω-bond angle on the effective 1D harmonic well at different temperatures.

Roughness Contributed by Different Water Models. By analytically solving the Smoluchowski equation (eq 1), Zwanzig[5] has shown previously that the diffusion coefficient, D, on an effective 1D landscape can be related to the underlying energetic roughness, ε, by

$$D = D_0 \exp[-(\varepsilon/k_B T)^\theta] \quad (4)$$

where D_0 is the diffusion coefficient on the smooth potential energy surface. Subsequently, it was shown that for a protein system in an effective 1D energy profile $\theta = 2$.[31,32] The quadratic dependence in eq 4 implies that the energetic roughness is random and has a Gaussian distribution. If $\theta = 1$, then the roughness is uniform and evenly distributed.[5]

From the diffusion coefficients, D, derived from fitting the autocorrelation function to an OU process at different temperatures, we obtained a plot of eq 4, as shown in Figure 3 for the simulations in the different water models[33] (i.e., TIP3P, SPC/E, TIP4P-Ew, and TIP5P) and also in vacuum.

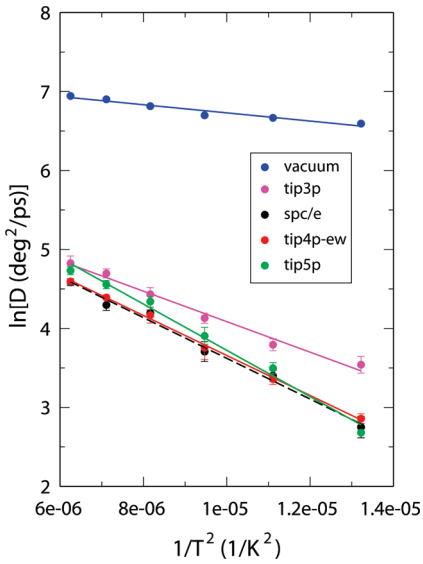

Figure 3. Temperature dependence of the effective diffusion coefficients of the ω-bond angle on the 1D harmonic well from simulations in four different water models and in vacuum. Linear fits using eq 4 with $\theta = 2$.

Table 1. Comparison of Energetic Roughness, Self-Diffusion Coefficients, and Structures of Different Water Models along with Intrinsic Roughness of the Peptide in Vacuum and Experimental Self-Diffusion Coefficient of Water

Water model	Roughness, ε (kcal/mol)	Self-diffusion coefficient (x 10^{-5} cm^2/s) at ~25°C and 1 atm	Structure of water model (A ball and stick model with partial charges on each charge center)
Vacuum	0.45	-	
TIP3P[34]	0.87	5.06[35] 5.65[36]	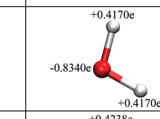
SPC/E[37]	1.01	2.49[35] 2.76[36]	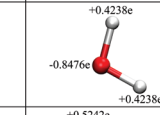
TIP4P-Ew[38,39]	1.00	2.4[38]	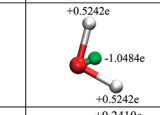
TIP5P[40]	1.08	2.62[35]	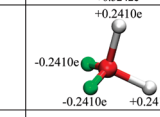
Experimental	-	2.23[41] 2.3[42,43]	

For each water model the data fitted very well with $\theta = 2$. By increasing the temperature range and carrying out simulations in TIP4P-EW at 600 K we further confirmed that $\theta = 2$ gives a better fit than $\theta = 1$. The plot of ln(D) versus $1/T^2$ (R^2=0.98) exhibited a higher correlation coefficient than ln(D) versus $1/T$ (R^2=0.93). Using $\theta = 2$ we calculated the roughness contributed by the different water models as well as the peptide's intrinsic roughness along the ω-bond angle in vacuum (the baseline) that are shown in Table 1. From Figure 3, it can be seen that the dynamics of the backbone ω angle is noticeably different in TIP3P than in SPC/E, TIP4P-Ew, and TIP5P, especially at lower temperature, i.e. the diffusion coefficients in TIP3P are higher as compared to those in other water models. The smaller contribution provided by TIP3P to the roughness results in faster dynamics at lower temperature. For the temperature range considered in this study, it is interesting to note the difference in backbone dynamics in the presence of different water models even at ambient to high temperatures.

If one considers the roughness of Ace-Ala-Pro-Nme in vacuum as the baseline, then TIP5P contributes ~0.63 kcal/mol of additional roughness to the energy landscape. TIP4P-EW and SPC/E contribute about ~0.56 kcal/mol. The roughness contributed by TIP3P (~0.42 kcal/mol) is the smallest. Therefore, SPC/E, TIP4P-EW, and TIP5P are slightly "rougher" than TIP3P. It is also important to note that the self-diffusion coefficient of TIP3P is about twice that of SPC/E, TIP4P-EW, and TIP5P (see Table 1), and the differences in energetic roughness can be partly attributed to that as well.

What Is the Main Contributing Factor to the Energetic Roughness by Water? By looking at the partial charges on the water models with three charged centers (SPC/E, TIP3P, and TIP4P-EW), one can see that the absolute magnitude of the partial charges is larger in SPC/E and TIP4P-EW than in TIP3P, and the increase correlates with a slight increase in the energetic roughness. This observation therefore raises the possibility that the majority of the contribution to the energetic roughness can be due to hydrogen bonding, which is electrostatic in nature in the classical definition of the water models. Alternatively, one can argue that the roughness may have an artificial component due to the Langevin thermostat and the random noise associated with it. However, it is important to note that the roughness is distinctly different for the different water models under similar conditions and using the same thermostat. Nonetheless, in order to test the effect of the Langevin thermostat on the energetic roughness, we doubled the collision frequency to 20 ps^{-1} and repeated the simulations for TIP4P-EW water. The diffusion coefficients obtained from these simulations at various temperatures are shown in Figure 4 (magenta). We clearly see, as expected at higher friction, that overall the dynamics is slightly slower compared to that obtained using a collision frequency of 10 ps^{-1} (Figure 4; red line). However, the slope of the line and hence the roughness is almost identical to simulations with a smaller collision frequency (Figure 4, compare red and magenta lines). Thus, changing the collision frequency or friction only affects D_0 in eq 4, as has also been observed earlier.[32]

Consequently, we hypothesize that the main source of energetic roughness is due to the forming and breaking of hydrogen bonding interactions between the water molecules, since the other nonbonded van der Waals interactions are far weaker. As noted above, the description of the hydrogen bonding interaction in the current classical model is purely electrostatic. Therefore, in order to test this hypothesis, we repeated the simulations of the peptide in a modified version of TIP4P-EW water, by zeroing all the partial charges only on the water molecules, thus eliminating the electrostatic interactions between the water molecules. The simulations

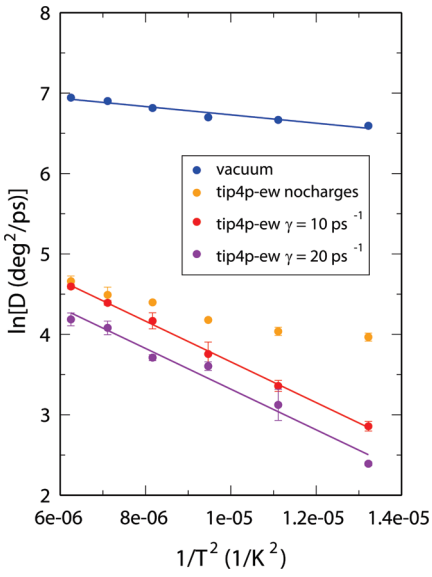

Figure 4. A plot of ln D versus $1/T^2$ for the simulations in vacuum and in TIP4P-EW when the collision frequency for the Langevin thermostat was set to 10 and 20 ps $^{-1}$ and when the partial charges were set to zero. Linear fits using eq 4 with $\theta = 2$.

were carried out with the same box sizes as those of the simulations with full partial charges at the different temperatures, in order to capture only the effect of eliminating the electrostatic interactions. For this model system of TIP4P-EW water with no partial charges, we clearly see that the slope of the line and hence the roughness also decreases considerably (Figure 4, orange) and is now comparable to that in vacuum. However, the data for TIP4P-EW with zero partial charges fitted eq 4 a little better with $\theta = 1$ (R^2=0.96) than with $\theta = 2$ (R^2=0.94), implying that without the electrostatic interactions the roughness is more uniform and evenly distributed. This change in the nature of the roughness can be attributed to the fact that van der Waals interactions are very short ranged and due only to the oxygen, since the radius of hydrogen for these water models is zero. On the other hand, electrostatic interactions are longer-ranged, and a slight change can have implications far away, adding to the randomness of this interaction.

Discussion and Concluding Remarks

We have investigated the effects of hydration on protein backbone motions and estimated the energetic roughness contributed by the most widely used water models on a quantitative level from all-atom MD simulations. We find that TIP3P water provides the least roughness resulting in the fastest dynamics of the ω-bond angle compared to that in other water models. This is not surprising since TIP3P has the highest translational diffusion coefficient ($\sim 5 \times 10^{-5}$ cm^2/s), which is more than double the self-diffusion coefficient of water ($\sim 2.3 \times 10^{-5}$ cm^2/s) estimated from experiments.[42] Similar behavior of the TIP3P water model has been observed in estimating the rotational diffusion of folded proteins using different atomistic simulation water models.[44] Furthermore, we note that all the other commonly used water models (SPC/E, TIP4P-Ew, TIP5P) considered in this study also have self-diffusion coefficients a little higher than that of water from experimental estimates. This means that protein dynamics with these water potentials will be slightly faster than in real water, and the energetic roughness provided by water may be slightly higher in reality than what it may appear from atomistic simulations. Hence real water may be slightly "rougher" than most of the simulation water models.

Interestingly, we also find that for the range of temperatures studied here (275 K-400 K) the dynamic behavior of protein backbone varies depending on the choice of the water model with the differences becoming more pronounced as temperatures are lowered. However, in contrast, a previous study of extremely low-temperature (20−300 K) behaviors of myoglobin solvated in TIP3P, TIP4P, and TIP5P has concluded that dynamic properties of proteins characterized by average mean-square displacements and time-averaged structures are similar irrespective of the choice of any TIP model.[45]

This work presents a very important and an additional property of water that can be taken into account while optimizing water potentials and, if need be, to reproduce experimental results. Such improved water potentials will help in more accurate simulations of protein motions. Our work also attempts to explain the underlying factors responsible for the roughness originating from the solvent. As depicted in Figure 5, the network of hydrogen bonds formed by water molecules around proteins constantly rearranges as the protein changes conformation. The water molecules immediately around the peptide form a transient, cagelike structure that is held together by the network of hydrogen bonds (Figure 5). As the conformation of the peptide changes, the hydrogen bonds break and reform to alter the network of hydrogen bonds. Each arrangement of the network of water molecules is an energetic substate of water and manifests itself as additional roughness on the underlying energy surface of proteins. The energetic roughness can have several implications for protein chemistry and motions. For example, when $\theta = 2$ in eq 4, the effect of the roughness on the dynamics of the protein can become very pronounced at low temperatures and restricts the motions of proteins. At higher temperature, when k_BT is much higher than the roughness (which is $\sim$1 kcal/mol), the effect of water molecules on the dynamics will be predominately due to the collision of the molecules and less due to the roughness of water.

Additionally, proteins that function as enzymes usually provide an environment in a cavity or binding site that is usually devoid of any appreciable amount of solvent. The effect of moving the substrate from the aqueous medium to the active site on the catalytic process is still not fully understood. However, this effect may only be limited to certain classes of enzymes,[46] like PPIases. From the above results, it can be suggested that the change in environment of the substrate can change the frictional drag as well as the topological features of the energy landscape of the substrate and thus "pave" the surface along the reaction coordinate for the conformational transition to occur. This

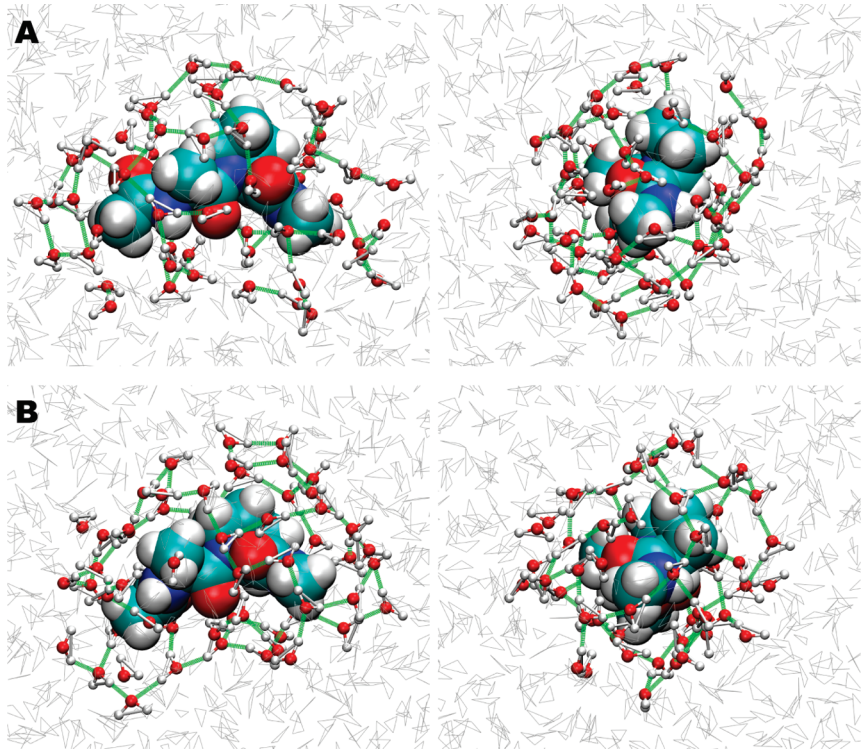

Figure 5. Hydrogen bonding network of the surrounding water molecules when the peptide Ace-Ala-Pro-Nme is in two different configurations (A and B). Each panel shows two different views of a configuration. The immediate water molecules surrounding this peptide are shown as balls and sticks (red and white), and the hydrogen bonds between the water molecules are shown as green. The remaining water molecules are shown as gray lines.

change in the topology of the landscape will most likely manifest itself by altering the kinetic pre-exponential factor. However, the dominating effect on the catalysis will still come from preorganization of the active site[47] and transition state stabilization, as shown for PPIases[48] or other energetic effects that are part of the exponential component of the kinetic rate equation. An indirect evidence for this effect is observed from the rate of *cis*−*trans* isomerization in different solvents. It can be clearly seen experimentally that the rate of isomerization is directly correlated with the solvents' self-diffusion coefficient,[24] which is inversely proportional to solvent friction.

In the current study, we have extracted information on peptide motions along one of the backbone torsional angles, i.e. ω-bond angle. In order to do so, we have used a simplified OU model by taking advantage of a good overdamped harmonic oscillator approximation of the dynamics. For such approximation to work, it is required that the degree of freedom in question has a Gaussian distribution. It will be interesting to investigate whether the same model can be applied to study peptide dynamics along other degrees of freedom and see how solvent alters those motions. It is possible that modified dynamic models may be required to reflect the characteristics of the free energy profiles along other degrees of freedom. A comparative study of water's contribution to the energetic roughness along various degrees of freedom may provide a clearer and more quantitative picture of the energy landscape of peptides. Moreover, such studies will also provide clues on how solvent affects the dynamics of folded proteins and the topological features of the potential energy landscape in the native well.

Computational Methods

Using the model peptide Ace-Ala-Pro-Nme we carried out a series of MD simulations in four widely used explicit simulation water models: TIP3P,[34] SPC/E,[37] TIP4P-EW,[38,39] and TIP5P.[40] For each water model, the simulations were performed at 275 K, 300 K, 325 K, 350 K, 375 K, and 400 K using the pmemd module in the AMBER 10 suite of programs[44] and the modified version[49] of the Cornell et al.[50] force field. The system was equilibrated at the set temperature and a constant pressure of 1 bar in a periodic cubic box with the edges of the box at least 10 Å away from the peptide. The temperature was regulated using the Langevin thermostat with a collision frequency of 10 ps^{-1}. Particle mesh Ewald[51] method was used to treat long-range interactions and all bonds involving hydrogen atoms were constrained by applying the SHAKE[52] algorithm. Three independent MD runs were carried out for 10 ns each at constant temperature and volume (NVT ensemble) using an integration time step of 2 fs for every combination of water model and temperature.

Acknowledgment. This work was supported in part by the National Science Foundation CAREER MCB-0953061 (D.H.) and Georgia Cancer Coalition (D.H.). This work was also supported by Georgia State's IBM System p5 supercomputer, acquired through a partnership of the Southeastern Universities Research Association and IBM supporting the SURAgrid initiative.

References

(1) Frauenfelder, H.; Sligar, S. G.; Wolynes, P. G. *Science* **1991**, *254*, 1598.

(2) Wales, D. J. *Energy landscapes*; Cambridge University Press: Cambridge, UK, New York, 2003.

(3) Frauenfelder, H.; Parak, F.; Young, R. D. *Annu. Rev. Biophys. Biophys. Chem.* **1988**, *17*, 451.

(4) Chaplin, M. *Nat. Rev. Mol. Cell Biol.* **2006**, *7*, 861.

(5) Zwanzig, R. *Proc. Natl. Acad. Sci. U. S. A.* **1988**, *85*, 2029.

(6) Hyeon, C.; Thirumalai, D. *Proc. Natl. Acad. Sci. U. S. A.* **2003**, *100*, 10249.

(7) Sagnella, D. E.; Straub, J. E.; Thirumalai, D. *J. Chem. Phys.* **2000**, *113*, 7702.

(8) Lapidus, L. J.; Eaton, W. A.; Hofrichter, J. *Proc. Natl. Acad. Sci. U. S. A.* **2000**, *97*, 7220.

(9) Nevo, R.; Brumfeld, V.; Kapon, R.; Hinterdorfer, P.; Reich, Z. *EMBO Rep.* **2005**, *6*, 482.

(10) Ohmine, I.; Saito, S. *Acc. Chem. Res.* **1999**, *32*, 741.

(11) Speedy, R. J.; Madura, J. D.; Jorgensen, W. L. *J. Phys. Chem.* **1987**, *91*, 909.

(12) Smith, J. D.; Cappa, C. D.; Wilson, K. R.; Messer, B. M.; Cohen, R. C.; Saykally, R. J. *Science* **2004**, *306*, 851.

(13) Smith, J. D.; Cappa, C. D.; Messer, B. M.; Cohen, R. C.; Saykally, R. J. *Science* **2005**, *308*, 793B.

(14) Nilsson, A.; Wernet, P.; Nordlund, D.; Bergmann, U.; Cavalleri, M.; Odelius, M.; Ogasawara, H.; Naslund, L. A.; Hirsch, T. K.; Glatzel, P.; Pettersson, L. G. M. *Science* **2005**, *308*, 793A.

(15) Chumaevskii, N. A.; Rodnikova, M. N. *J. Mol. Liq.* **2003**, *106*, 167.

(16) Head-Gordon, T.; Johnson, M. E. *Proc. Natl. Acad. Sci. U. S. A.* **2006**, *103*, 7973.

(17) Markovitch, O.; Agmon, N. *Mol. Phys.* **2008**, *106*, 485.

(18) Myneni, S.; Luo, Y.; Naslund, L. A.; Cavalleri, M.; Ojamae, L.; Ogasawara, H.; Pelmenschikov, A.; Wernet, P.; Vaterlein, P.; Heske, C.; Hussain, Z.; Pettersson, L. G. M.; Nilsson, A. *J. Phys.: Condens. Matter* **2002**, *14*, L213.

(19) Wernet, P.; Nordlund, D.; Bergmann, U.; Cavalleri, M.; Odelius, M.; Ogasawara, H.; Naslund, L. A.; Hirsch, T. K.; Ojamae, L.; Glatzel, P.; Pettersson, L. G. M.; Nilsson, A. *Science* **2004**, *304*, 995.

(20) Fenimore, P. W.; Frauenfelder, H.; McMahon, B. H.; Parak, F. G. *Proc. Natl. Acad. Sci. U. S. A.* **2002**, *99*, 16047.

(21) Frauenfelder, H.; Chen, G.; Berendzen, J.; Fenimore, P. W.; Jansson, H.; McMahon, B. H.; Stroe, I. R.; Swenson, J.; Young, R. D. *Proc. Natl. Acad. Sci. U. S. A.* **2009**, *106*, 5129.

(22) Dill, K. A. *Biochemistry* **1990**, *29*, 7133.

(23) Fanghanel, J.; Fischer, G. *Front. Biosci.* **2004**, *9*, 3453.

(24) Eberhardt, E. S.; Loh, S. N.; Hinck, A. P.; Raines, R. T. *J. Am. Chem. Soc.* **1992**, *114*, 5437.

(25) Ikura, T.; Kinoshita, K.; Ito, N. *Protein Eng. Des. Sel.* **2008**, *21*, 83.

(26) Lu, K. P.; Finn, G.; Lee, T. H.; Nicholson, L. K. *Nat. Chem. Biol.* **2007**, *3*, 619.

(27) Brandts, J. F.; Halvorson, H. R.; Brennan, M. *Biochemistry* **1975**, *14*, 4953.

(28) Wedemeyer, W. J.; Welker, E.; Scheraga, H. A. *Biochemistry* **2002**, *41*, 14637.

(29) Doshi, U.; Hamelberg, D. *J. Phys. Chem. B* **2009**, *113*, 16590.

(30) Wang, M. C.; Uhlenbeck, G. E. *Rev. Mod. Phys.* **1945**, *17*, 20.

(31) Hamelberg, D.; Shen, T.; Andrew McCammon, J. *J. Chem. Phys.* **2005**, *122*, 241103.

(32) Hamelberg, D.; Shen, T.; McCammon, J. A. *J. Chem. Phys.* **2006**, *125*, 094905.

(33) Guillot, B. *J. Mol. Liq.* **2002**, *101*, 219.

(34) Jorgensen, W. L.; Chandrasekhar, J.; Madura, J. D.; Impey, R. W.; Klein, M. L. *J. Chem. Phys.* **1983**, *79*, 926.

(35) Mahoney, M. W.; Jorgensen, W. L. *J. Chem. Phys.* **2001**, *114*, 363.

(36) Mark, P.; Nilsson, L. *J. Phys. Chem. A* **2001**, *105*, 9954.

(37) Berendsen, H. J. C.; Grigera, J. R.; Straatsma, T. P. *J. Phys. Chem.* **1987**, *91*, 6269.

(38) Horn, H. W.; Swope, W. C.; Pitera, J. W.; Madura, J. D.; Dick, T. J.; Hura, G. L.; Head-Gordon, T. *J. Chem. Phys.* **2004**, *120*, 9665.

(39) Jorgensen, W. L.; Madura, J. D. *Mol. Phys.* **1985**, *56*, 1381.

(40) Mahoney, M. W.; Jorgensen, W. L. *J. Chem. Phys.* **2000**, *112*, 8910.

(41) Gillen, K. T.; Douglas, D. C.; Hoch, M. J. R. *J. Chem. Phys.* **1972**, *57*, 5117.

(42) Holz, M.; Heil, S. R.; Sacco, A. *Phys. Chem. Chem. Phys.* **2000**, *2*, 4740.

(43) Price, W. S.; Ide, H.; Arata, Y. *J. Phys. Chem. A* **1999**, *103*, 448.

(44) Case, D. A.; Darden, T. A.; Cheatham, T. E., III; Simmerling, C. L.; Wang, J.; Duke, R. E.; Luo, R.; Crowley, M.; Walker, R. C.; Zhang, W.; Merz, K. M.; Wang, B.; Hayik, S.; Roitberg, A.; Seabra, G.; Kolossváry, I.; Wong, K. F.; Paesani, F.; Vanicek, J.; Wu, X.; Brozell, S. R.; Steinbrecher, T.; Gohlke, H.; Yang, L.; Tan, C.; Mongan, J.; Hornak, V.; Cui, G.; Mathews, D. H.; Seetin, M. G.; Sagui, C.; Babin, V.; Kollman, P. A. AMBER 10. In *AMBER 10*; University of California: San Francisco, 2008.

(45) Glass, D. C.; Krishnan, M.; Nutt, D. R.; Smith, J. C. *J. Chem. Theory Comput.* **2010**, *6*, 1390.

(46) Warshel, A.; Aqvist, J.; Creighton, S. *Proc. Natl. Acad. Sci. U. S. A.* **1989**, *86*, 5820.

(47) Warshel, A. *Proc. Natl. Acad. Sci. U. S. A.* **1978**, *75*, 5250.

(48) Hamelberg, D.; McCammon, J. A. *J. Am. Chem. Soc.* **2009**, *131*, 147.

(49) Hornak, V.; Abel, R.; Okur, A.; Strockbine, B.; Roitberg, A.; Simmerling, C. *Proteins* **2006**, *65*, 712.

(50) Cornell, W. D.; Cieplak, P.; Bayly, C. I.; Gould, I. R.; Merz, K. M.; Ferguson, D. M.; Spellmeyer, D. C.; Fox, T.; Caldwell, J. W.; Kollman, P. A. *J. Am. Chem. Soc.* **1995**, *117*, 5179.

(51) Darden, T.; York, D.; Pedersen, L. *J. Chem. Phys.* **1993**, *98*, 10089.

(52) Ryckaert, J.; Cicotti, G.; Berendsen, H. *J. Comput. Phys.* **1977**, *23*, 327.

CT100183S